Received January 20, 2021, accepted January 30, 2021, date of publication February 5, 2021, date of current version June 22, 2021.

Digital Object Identifier 10.1109/ACCESS.2021.3057454

A Wave Peak Frequency Tracking Method Based on Two-Stage Recursive Extended Least Squares Identification Algorithm

JIANPING YUAN[1,2], SHUN AN[3], XINXIANG PAN[1], HONGFEI MAO[1], AND LONGJIN WANG[3]

[1]College of Ocean Engineering, Guangdong Ocean University, Zhanjiang 524088, China
[2]College of Ship Engineering, Harbin Engineering University, Harbin 150001, China
[3]College of Electromechanical Engineering, Qingdao University of Science and Technology, Qingdao 266061, China

Corresponding author: Longjin Wang (wljwlj1984@126.com)

This work was supported by the State Administration of Science, Technology and Industry for National Defence under Grant JCKYS2019604SXJQR-02.

ABSTRACT This paper proposes the wave peak frequency tracking methods based on the least squares identification algorithm. The wave disturbance model is transformed into an autoregressive moving average (ARMA) model and a recursive extended least squares (RELS) algorithm is derived to identify the model parameters by using the auxiliary model identification idea. Furthermore, a two-stage recursive extended least squares (2S-RELS) algorithm is presented to improve the convergence speed by using the hierarchical identification principle. A ship heading control system with the wave peak frequency tracker is built to evaluate the effectiveness of the proposed algorithms. Finally, simulation results show that the proposed algorithms can estimate the wave peak frequency accurately and the 2S-RELS algorithm can improve the convergence speed effectively.

INDEX TERMS Wave frequency tracker, least squares, recursive identification, hierarchical identification.

I. INTRODUCTION

When a ship is sailing in a sea way, the manoeuvring characteristics are influenced by external forces and moments caused by waves [1]. In order to increase the safety and performance of the ship control system, a filter based on the wave peak frequency tracker is necessary to eliminate the effect of the wave disturbances. To describe the wave spectrum in different sea state accurately, both linear and nonlinear models were proposed [2], [3]. Among the proposed descriptions of the wave spectrum, the 2nd-order linear wave disturbance model which is applied to fit the shape of the PM spectrum is widely used for filter design [4]. However, as the sea state and navigation state vary constantly, the peak frequency of the wave spectrum is modified by the wave encounter frequency which varies with the wave state, the total speed of the ship and the angle between the heading and the direction of the wave, which leads to the difficulty of wave filter design [5]. Many methods have been proposed to estimate the wave encounter frequency [6], [7]. Belleter *et al.* proposed a signal based nonlinear wave encounter frequency estimator which is proved to be global exponential stable and the estimates of the wave encounter frequency for both regular and irregular waves confirmed the result by experimental analysis [8].

System identification is the theory and methods of establishing the mathematical models, which are the basis of system analysis, controller design, signal processing and filtering [9]–[12]. The recursive least squares (RLS) algorithms are suitable for on-line parameter estimation [13]. Wang *et al.* studied the parameter identification problems for a class of nonlinear stochastic systems with colored noise based on the recursive least squares parameter estimation algorithms [14]. Ding proposed a combined state and least squares parameter estimation algorithm for an observer canonical state space system [15].

The auxiliary model identification idea is widely applied to deal with the identification issues in the presence of the unmeasurable variables in the information vectors [16], [17]. For example, Wang *et al.* proposed an auxiliary model based recursive least squares algorithm for a class of linear-in-parameters output error moving average systems [18] and Chen *et al.* presented an auxiliary model based extended stochastic gradient algorithm for multiple-input multiple-output (MIMO) system using the multi-innovation

The associate editor coordinating the review of this manuscript and approving it for publication was Jing Yan.

identification theory [19]. Since the derived identification model contains unmeasurable terms, the auxiliary model based parameter estimate algorithms were presented to handle this issue. The hierarchical identification principle is introduced to transform a large-scale system into several fictitious subsystems with small size to reduce the computational burden [20], [21]. Guo *et al.* presented the auxiliary model based hierarchical estimation algorithms for bilinear stochastic systems with colored noises [22]. Ding *et al.* proposed a three-stage recursive least squares parameter identification algorithm for Hammerstein nonlinear system using the hierarchical identification principle [23].

The wave filter is important for the dynamic positioning (DP) system [24], [25] and the ship autopilot system [26]. This is applied such that only the low-frequency (LF) components of a ship are considered by the control system and the high-frequency (HF) components, also known as wave-frequency (WF) disturbance which can increase the fuel consumption and the wear of mechanical equipment, need to be prevented to enter the control loop [27]–[29]. During the past decades, many wave filter design methods have been proposed [30]–[32]. Fossen and Perez gave an overview of Kalman filter design for the DP and autopilot system [33]. Deng *et al.* proposed a modified adaptive observer based backstepping control algorithm for the dynamic positioning system [34]. Yang *et al.* presented a trajectory tracking robust controller and disturbance observer to deal with external disturbances and nonlinear terms [35]. In [36], an adaptive disturbance observer is proposed to solve the robust trajectory tracking problem for underwater vehicles in presence of unknown external disturbances and parametric uncertainties.

An online identification method of the wave peak frequency is proposed based on the recursive extended least squares (RELS) algorithm by using the auxiliary model identification idea. Furthermore, a two-stage recursive extended least squares (2S-RELS) algorithm is presented to reduce the computational burden by using the hierarchical identification principle. The main contributions of this paper are as follows.

- The wave disturbance model is expressed as an ARMA model for the wave peak frequency identification and a RELS algorithm is presented to identify the wave peak frequency by using the auxiliary model identification idea.
- A 2S-RELS algorithm is presented to reduce the computational burden and improve the convergence speed by using the hierarchical identification principle.

The structure of this paper is as follows. Section II describes the identification model of the 2nd-order linear wave disturbance model. Section III proposes a RELS algorithm by using the auxiliary model identification idea. Section IV derives a 2S-RELS algorithm by using the auxiliary model identification idea and the hierarchical identification principle, respectively. The wave peak frequency computation method based on the identified parameters is given in section V. A ship heading control system is built by using the wave peak frequency tracker and the effectiveness of the proposed algorithms is verified by simulations in Section VI. Finally, we offer some concluding remarks in Section VII.

II. 2nd-ORDER LINEAR WAVE DISTURBANCE MODEL

Let us define some notations first. "$X := A$" stands for "A is defined as X"; I_n denotes an identity matrix of size $n \times n$; 1_n denotes a $n \times 1$ vector whose elements are all unity; z denotes a uint forward shift operator with $zx(t) = x(t+1)$ and $z^{-1}x(t) = x(t-1)$. The 2nd-order linear wave disturbance model due to the 1st-order wave disturbances is usually described by the following transfer function:

$$\psi_\omega(s) = \frac{K_\omega s}{s^2 + 2\xi\omega_0 s + \omega_0^2} v(s), \tag{1}$$

where $v(s)$ is the zero-mean Gaussian white noise process, $\psi_\omega(s)$ is the wave frequency motion due to the 1st-order wave disturbances, K_ω is a constant gain describing the wave excitation intensity, ξ is a relative damping ratio and ω_0 is the wave peak frequency. For a ship moving with the forward speed U, the wave frequency ω_0 is modified by the wave encounter frequency ω_e according to

$$\omega_e = \omega_0 - \frac{\omega_0^2}{g} U \cos(\beta), \tag{2}$$

where β is the angle between the heading and the direction of the wave, and g is the acceleration of gravity.

However, in practice, $\psi_\omega(s)$ cannot be measured directly since both the LF ship motion $\psi(s)$ and HF wave induced motion $\psi_\omega(s)$ are included in the measurement of a compass $\psi_{tot}(s)$ as seen in Figure 1, that is:

$$\psi_{tot}(s) = \psi(s) + \psi_\omega(s). \tag{3}$$

In order to acquire the HF motion component data, a high-pass filter $h_{HP}(s)$ could be applied to separate $\psi_\omega(s)$ from the measurement by using a filtered signal $\bar{\psi}_\omega(s)$. Therefore, an approximation of $\psi_\omega(s)$ can be obtained by:

$$\bar{\psi}_\omega(s) = h_{HP}(s)\psi_{tot}(s), \tag{4}$$

where the cut-off frequency of the high-pass filter should be lower than the wave encounter frequency. The high-pass

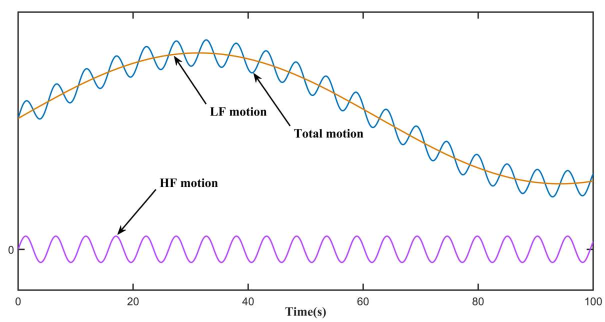

FIGURE 1. Illustration of total, LF, and HF motion of the ship heading.

filter will weaken the LF motion components generated by the control input $u(s)$ if the following condition can be fullfilled:

$$h_{HP}(s)\psi(s) = h_{HP}(s)h_{ship}(s)u(s) \ll 1. \tag{5}$$

In order to establish the identification model, the 2nd-order linear wave disturbance model can be expressed as an ARMA model according to [2]

$$A(z^{-1})\psi_\omega(k) = B(z^{-1})v(k), \tag{6}$$

where

$$A(z^{-1}) := 1 + a_1z^{-1} + a_2z^{-2}, \tag{7}$$
$$B(z^{-1}) := 1 + b_1z^{-1}. \tag{8}$$

According to (1) and (6), we obtain the following relationship:

$$\psi_\omega(t) = -a_1\psi_\omega(t-1) - a_2\psi_\omega(t-2) + b_1v(t-1) + v(t). \tag{9}$$

Replacing $\psi_\omega(s)$ in (9) with its approximate value $\bar{\psi}_\omega(s)$, we can obtain the following representation:

$$\bar{\psi}_\omega(t) = -a_1\bar{\psi}_\omega(t-1) - a_2\bar{\psi}_\omega(t-2) + b_1v(t-1) + v(t). \tag{10}$$

Let y be equal to $\bar{\psi}_\omega$ and Equation (10) can be rewritten as:

$$\begin{aligned} y(t) &= \boldsymbol{\varphi}_s^{\mathrm{T}}(t)\boldsymbol{\theta}_s + \varphi_n(t)\theta_n + v(t) &(11)\\ &= \boldsymbol{\varphi}^{\mathrm{T}}(t)\boldsymbol{\theta} + v(t), &(12)\end{aligned}$$

where

$$\begin{aligned} \boldsymbol{\theta}_s^{\mathrm{T}} &:= [a_1, a_2] \in \mathbb{R}^{n_1},\\ \theta_n &:= b_1 \in \mathbb{R}^{n_2},\\ \boldsymbol{\theta}^{\mathrm{T}} &:= [\boldsymbol{\theta}_s^{\mathrm{T}}, \theta_n] \in \mathbb{R}^{n_0},\\ \varphi_n(t) &:= v(t-1) \in \mathbb{R}^{n_2},\\ \boldsymbol{\varphi}_s^{\mathrm{T}}(t) &:= [-y(t-1), -y(t-2)] \in \mathbb{R}^{n_1},\\ \boldsymbol{\varphi}^{\mathrm{T}}(t) &:= [\boldsymbol{\varphi}_s^{\mathrm{T}}(t), \varphi_n(t)] \in \mathbb{R}^{n_0}, \end{aligned}$$

where $\boldsymbol{\theta}_s$ and $\boldsymbol{\theta}$ are the parameter vectors to be identified, $\boldsymbol{\varphi}_s$ and $\boldsymbol{\varphi}(t)$ are the information vectors.

The proposed parameter estimation algorithms in this paper are based on this identification model in (12). Many identification methods are derived based on the identification models of the systems [37]–[41] and can be used to estimate the parameters of other linear systems and nonlinear systems [42]–[46], and can be applied to literatures [47]–[51] such as chemical process control systems. The objective of this paper is to develop new recursive identification algorithms to estimate the parameters of the wave disturbance model and calculate the wave peak frequency on-line.

III. THE RECURSIVE EXTENDED LEAST SQUARES ALGORITHM

In this section, a RELS algorithm is proposed based on the input-output representation of the 2nd-order linear wave disturbance model by using the auxiliary model identification idea.

Use the input-output data to define the stacked vector $\boldsymbol{Y}_t$ and the stacked matrix $\boldsymbol{\Phi}_t$ as

$$\boldsymbol{Y}_t := \begin{bmatrix} y(1)\\ y(2)\\ \vdots\\ y(t)\end{bmatrix} \in \mathbb{R}^t, \quad \boldsymbol{\Phi}_t := \begin{bmatrix} \boldsymbol{\varphi}^{\mathrm{T}}(1)\\ \boldsymbol{\varphi}^{\mathrm{T}}(2)\\ \vdots\\ \boldsymbol{\varphi}^{\mathrm{T}}(t)\end{bmatrix} \in \mathbb{R}^{t\times 3}.$$

According to (12), define a quadratic criterion function:

$$J_1(\boldsymbol{\theta}) := \| \boldsymbol{Y}_t - \boldsymbol{\Phi}_t\boldsymbol{\theta} \|^2 . \tag{13}$$

Minimizing $J_1(\boldsymbol{\theta})$ and letting its partial derivative with respect to $\boldsymbol{\theta}$ be zero, we can obtain the recursive relations of computing $\hat{\boldsymbol{\theta}}(t)$:

$$\hat{\boldsymbol{\theta}}(t) = \hat{\boldsymbol{\theta}}(t-1) + \boldsymbol{L}(t)[y(t) - \boldsymbol{\varphi}^{\mathrm{T}}(t)\hat{\boldsymbol{\theta}}(t-1)], \tag{14}$$
$$\boldsymbol{L}(t) = \frac{\boldsymbol{P}(t-1)\boldsymbol{\varphi}(t)}{1+\boldsymbol{\varphi}^{\mathrm{T}}(t)\boldsymbol{P}(t-1)\boldsymbol{\varphi}(t)}, \tag{15}$$
$$\boldsymbol{P}(t) = [\boldsymbol{I}_3 - \boldsymbol{L}(t)\boldsymbol{\varphi}^{\mathrm{T}}(t)]\boldsymbol{P}(t-1). \tag{16}$$

However, the information vector $\boldsymbol{\varphi}(t)$ in (12) contains the unmeasurable term $\varphi_n(t)$, and then Equation (14) cannot give the estimate $\hat{\boldsymbol{\theta}}(t)$ directly. The solution is to replace the unknown item $\varphi_n(t)$ in $\boldsymbol{\varphi}(t)$ with its corresponding estimate $\hat{\varphi}_n(t)$.

From (12), we have $v(t) = y(t) - \boldsymbol{\varphi}^{\mathrm{T}}(t)\boldsymbol{\theta}$. Replacing $\boldsymbol{\varphi}(t)$ and $\boldsymbol{\theta}$ with $\hat{\boldsymbol{\varphi}}(t)$ and $\hat{\boldsymbol{\theta}}(t)$, respectively, the estimate of $v(t)$ can be computed by

$$\hat{v}(t) = y(t) - \hat{\boldsymbol{\varphi}}^{\mathrm{T}}(t)\hat{\boldsymbol{\theta}}(t). \tag{17}$$

Replacing $\boldsymbol{\varphi}(t)$ in (14)–(16) with its estimate $\hat{\boldsymbol{\varphi}}(t)$, we can derive the following recursive least squares relations:

$$\hat{\boldsymbol{\theta}}(t) = \hat{\boldsymbol{\theta}}(t-1) + \boldsymbol{L}(t)[y(t) - \hat{\boldsymbol{\varphi}}^{\mathrm{T}}(t)\hat{\boldsymbol{\theta}}(t-1)], \tag{18}$$
$$\boldsymbol{L}(t) = \frac{\boldsymbol{P}(t-1)\hat{\boldsymbol{\varphi}}(t)}{1+\hat{\boldsymbol{\varphi}}^{\mathrm{T}}(t)\boldsymbol{P}(t-1)\hat{\boldsymbol{\varphi}}(t)}, \tag{19}$$
$$\boldsymbol{P}(t) = [\boldsymbol{I}_3 - \boldsymbol{L}(t)\hat{\boldsymbol{\varphi}}^{\mathrm{T}}(t)]\boldsymbol{P}(t-1). \tag{20}$$

Combining (17)–(20), we can summarize the recursive extended least squares (RELS) algorithm for the 2nd-order linear wave disturbance model as

$$\hat{\boldsymbol{\theta}}(t) = \hat{\boldsymbol{\theta}}(t-1) + \boldsymbol{L}(t)[y(t) - \hat{\boldsymbol{\varphi}}^{\mathrm{T}}(t)\hat{\boldsymbol{\theta}}(t-1)], \tag{21}$$
$$\boldsymbol{L}(t) = \frac{\boldsymbol{P}(t-1)\hat{\boldsymbol{\varphi}}(t)}{1+\hat{\boldsymbol{\varphi}}^{\mathrm{T}}(t)\boldsymbol{P}(t-1)\hat{\boldsymbol{\varphi}}(t)}, \tag{22}$$
$$\boldsymbol{P}(t) = [\boldsymbol{I}_3 - \boldsymbol{L}(t)\hat{\boldsymbol{\varphi}}^{\mathrm{T}}(t)]\boldsymbol{P}(t-1), \tag{23}$$
$$\hat{\boldsymbol{\varphi}}(t) = \begin{bmatrix} \boldsymbol{\varphi}_s(t)\\ \hat{\varphi}_n(t)\end{bmatrix}, \tag{24}$$
$$\hat{\varphi}_n(t) = \hat{v}(t-1), \tag{25}$$

TABLE 1. The flop amounts of the RELS algorithm.

Algorithm	Computational sequences	Multiplications	Additions
$\hat{\boldsymbol{\theta}}(t)$	$\hat{\boldsymbol{\theta}}(t)=\hat{\boldsymbol{\theta}}(t-1)+\boldsymbol{L}(t)e(t)]$	n_0	n_0
	$e(t):=y(t)-\hat{\boldsymbol{\varphi}}^{\mathrm{T}}(t)\hat{\boldsymbol{\theta}}(t-1)$	n_0	n_0
$\boldsymbol{L}(t)$	$\boldsymbol{L}(t)=\boldsymbol{\chi}(t)[1+\hat{\boldsymbol{\varphi}}^{\mathrm{T}}(t)\boldsymbol{P}(t-1)\hat{\boldsymbol{\varphi}}(t)]^{-1}$	$2n_0$	n_0
	$\boldsymbol{\chi}(t):=\boldsymbol{P}(t-1)\hat{\boldsymbol{\varphi}}(t)$	n_0^2	$n_0(n_0-1)$
$\boldsymbol{P}(t)$	$\boldsymbol{P}(t)=\boldsymbol{P}(t-1)-\boldsymbol{L}(t)\boldsymbol{\chi}^{\mathrm{T}}(t)$	n_0^2	n_0^2
$\hat{v}(t)$	$\hat{v}(t)=y(t)-\hat{\boldsymbol{\varphi}}^{\mathrm{T}}(t)\hat{\boldsymbol{\theta}}(t)$	n_0	n_0
Sum		$2n_0^2+5n_0$	$2n_0^2+3n_0$
Total flops		$N_1:=4n_0^2+8n_0$	

$$\boldsymbol{\varphi}_s(t)=[-y(t-1),-y(t-2)]^{\mathrm{T}}, \tag{26}$$
$$\hat{v}(t)=y(t)-\hat{\boldsymbol{\varphi}}^{\mathrm{T}}(t)\hat{\boldsymbol{\theta}}(t). \tag{27}$$

The multiplications and additions of the RELS algorithm is given in Table 1. The computation procedures of the RELS algorithm in (21)–(27) are listed in the following.

1) Initialize: let $t=3$, $\hat{\boldsymbol{\theta}}(0)=1_3/p_0$, $\boldsymbol{P}(0)=p_0\boldsymbol{I}_3$, $\hat{v}(t-1)=0$, and p_0 is taken to be a large number, e.g., $p_0=10^6$.
2) Collect the output data $y(t)$. Form $\boldsymbol{\varphi}_s(t)$ and $\hat{\boldsymbol{\varphi}}(t)$ by (26) and (24), respectively.
3) Compute the gain vector $\boldsymbol{L}(t)$ by (22) and the covariance matrix $\boldsymbol{P}(t)$ by (23).
4) Update the parameter estimate $\hat{\boldsymbol{\theta}}(t)$ by (21).
5) Compute $\hat{v}(t)$ by (27).
6) Increase t by 1 and go to Step 2.

IV. THE TWO-STAGE RELS ALGORITHM

In order to improve the convergence speed, the ARMA model of the wave disturbance is decomposed into two fictitious subsystems and the 2S-RELS algorithm is applied to identify the wave peak frequency. Define two intermediate variables:

$$y_1(t):=y(t)-\varphi_n(t)\theta_n, \tag{28}$$
$$y_2(t):=y(t)-\boldsymbol{\varphi}_s^{\mathrm{T}}(t)\boldsymbol{\theta}_s. \tag{29}$$

Based on the hierarchical identification principle, and from (6), we can obtain two subsystems:

$$y_1(t)=\boldsymbol{\varphi}_s^{\mathrm{T}}(t)\boldsymbol{\theta}_s+v(t), \tag{30}$$
$$y_2(t)=\varphi_n(t)\theta_n+v(t). \tag{31}$$

From (30) and (31), define two quadratic criterion functions:

$$J_2(\boldsymbol{\theta}_s):=\sum_{i=1}^{t}\|y_1(i)-\boldsymbol{\varphi}_s^{\mathrm{T}}(i)\boldsymbol{\theta}_s\|^2, \tag{32}$$
$$J_3(\theta_n):=\sum_{i=1}^{t}\|y_2(i)-\varphi_n(i)\theta_n\|^2. \tag{33}$$

Minimizing the quadratic criterion functions $J_2(\boldsymbol{\theta}_s)$ and $J_3(\theta_n)$, and letting their partial derivatives with respect to $\boldsymbol{\theta}_s$ and θ_n be zero, we can obtain the recursive relations to compute $\hat{\boldsymbol{\theta}}_s(t)$ and $\hat{\theta}_n(t)$:

$$\hat{\boldsymbol{\theta}}_s(t)=\hat{\boldsymbol{\theta}}_s(t-1)+\boldsymbol{L}_s(t)[y_1(t)-\boldsymbol{\varphi}_s^{\mathrm{T}}(t)\hat{\boldsymbol{\theta}}_s(t-1)], \tag{34}$$
$$\boldsymbol{L}_s(t)=\frac{\boldsymbol{P}_s(t-1)\boldsymbol{\varphi}_s(t)}{1+\boldsymbol{\varphi}_s^{\mathrm{T}}(t)\boldsymbol{P}_s(t-1)\boldsymbol{\varphi}_s(t)}, \tag{35}$$
$$\boldsymbol{P}_s(t)=[\boldsymbol{I}_2-\boldsymbol{L}_s(t)\boldsymbol{\varphi}_s^{\mathrm{T}}(t)]\boldsymbol{P}_s(t-1), \tag{36}$$
$$\hat{\theta}_n(t)=\hat{\theta}_n(t-1)+L_n(t)[y_2(t)-\varphi_n(t)\hat{\theta}_n(t-1)], \tag{37}$$
$$L_n(t)=\frac{P_n(t-1)\varphi_n(t)}{1+P_n(t-1)\varphi_n^2(t)}, \tag{38}$$
$$P_n(t)=[1-L_n(t)\varphi_n(t)]P_n(t-1). \tag{39}$$

Substituting (28) into (34) and (29) into (37), we have the following relations:

$$\begin{aligned}\hat{\boldsymbol{\theta}}_s(t)&=\hat{\boldsymbol{\theta}}_s(t-1)+\boldsymbol{L}_s(t)\\&\quad\times[y(t)-\varphi_n(t)\theta_n-\boldsymbol{\varphi}_s^{\mathrm{T}}(t)\hat{\boldsymbol{\theta}}_s(t-1)],\end{aligned} \tag{40}$$
$$\begin{aligned}\hat{\theta}_n(t)&=\hat{\theta}_n(t-1)+L_n(t)\\&\quad\times[y(t)-\boldsymbol{\varphi}_s^{\mathrm{T}}(t)\boldsymbol{\theta}_s-\varphi_n(t)\hat{\theta}_n(t-1)].\end{aligned} \tag{41}$$

Similarly, the right-hand sides of (40) and (41) contain the unknown parameter vectors $\boldsymbol{\theta}_s$ and θ_n, and φ_n is the unmeasured noise term, so Equation (40) and (41) cannot give the estimates $\hat{\boldsymbol{\theta}}_s(t)$ and $\hat{\theta}_n(t)$ directly. The solution is to replace $\boldsymbol{\theta}_s$, θ_n and $\varphi_n(t)$ with their corresponding estimates. From (12), we have $v(t)=y(t)-\boldsymbol{\varphi}^{\mathrm{T}}(t)\boldsymbol{\theta}$. Replacing $\boldsymbol{\varphi}(t)$ and $\boldsymbol{\theta}$ with $\hat{\boldsymbol{\varphi}}(t)$ and $\hat{\boldsymbol{\theta}}(t)$, respectively, the estimate of $v(t)$ can be computed by

$$\hat{v}(t)=y(t)-\hat{\boldsymbol{\varphi}}^{\mathrm{T}}(t)\hat{\boldsymbol{\theta}}(t). \tag{42}$$

Replacing $\varphi_n(t)$ and θ_n in (40) with their estimates $\hat{\varphi}_n(t)$ and $\hat{\theta}_n(t-1)$, and replacing $\varphi_n(t)$ and $\boldsymbol{\theta}_s$ in (41) with their estimates $\hat{\varphi}_n(t)$ and $\hat{\boldsymbol{\theta}}_s(t-1)$, we can summarize the 2S-RELS algorithm for estimating θ_n and $\boldsymbol{\theta}_s$ of the 2nd-order linear wave disturbance model as:

$$\begin{aligned}\hat{\boldsymbol{\theta}}_s(t)&=\hat{\boldsymbol{\theta}}_s(t-1)+\boldsymbol{L}_s(t)[y(t)\\&\quad-\hat{\varphi}_n(t)\hat{\theta}_n(t-1)-\boldsymbol{\varphi}_s^{\mathrm{T}}(t)\hat{\boldsymbol{\theta}}_s(t-1)],\end{aligned} \tag{43}$$
$$\begin{aligned}\hat{\theta}_n(t)&=\hat{\theta}_n(t-1)+L_n(t)[y(t)\\&\quad-\boldsymbol{\varphi}_s^{\mathrm{T}}(t)\hat{\boldsymbol{\theta}}_s(t-1)-\hat{\varphi}_n(t)\hat{\theta}_n(t-1)],\end{aligned} \tag{44}$$
$$\boldsymbol{L}_s(t)=\frac{\boldsymbol{P}_s(t-1)\boldsymbol{\varphi}_s(t)}{1+\boldsymbol{\varphi}_s^{\mathrm{T}}(t)\boldsymbol{P}_s(t-1)\boldsymbol{\varphi}_s(t)}, \tag{45}$$
$$\boldsymbol{P}_s(t)=[\boldsymbol{I}_2-\boldsymbol{L}_s(t)\boldsymbol{\varphi}_s^{\mathrm{T}}(t)]\boldsymbol{P}_s(t-1), \tag{46}$$
$$L_n(t)=\frac{P_n(t-1)\hat{\varphi}_n(t)}{1+P_n(t-1)\hat{\varphi}_n{}^2(t)}, \tag{47}$$
$$P_n(t)=[1-L_n(t)\hat{\varphi}_n(t)]P_n(t-1), \tag{48}$$
$$\hat{v}(t)=y(t)-\hat{\boldsymbol{\varphi}}^{\mathrm{T}}(t)\hat{\boldsymbol{\theta}}(t), \tag{49}$$
$$\boldsymbol{\varphi}_s^{\mathrm{T}}(t)=[-y(t-1),-y(t-2)], \tag{50}$$
$$\hat{\varphi}_n(t)=\hat{v}(t-1). \tag{51}$$

TABLE 2. The flop amounts of the 2S-RELS algorithm.

Algorithm	Computational sequences	Multiplications	Additions
$\hat{\boldsymbol{\theta}}_s(t)$	$\hat{\boldsymbol{\theta}}_s(t) = \hat{\boldsymbol{\theta}}_s(t-1) + \boldsymbol{L}_s(t)e(t)$	n_1	n_1
	$e(t) := y(t) - \boldsymbol{\varphi}_s^{\mathrm{T}}(t)\hat{\boldsymbol{\theta}}_s(t-1) - \hat{\varphi}_n(t)\hat{\theta}_n(t-1)$	n_0	n_0
$\boldsymbol{L}_s(t)$	$\boldsymbol{L}_s(t) = \boldsymbol{\chi}_s(t)[1 + \boldsymbol{\varphi}_s^{\mathrm{T}}(t)\boldsymbol{\chi}_s(t)]^{-1}$	$2n_1$	n_1
	$\boldsymbol{\chi}_s(t) := \boldsymbol{P}_s(t-1)\boldsymbol{\varphi}_s(t)$	n_1^2	$n_1(n_1-1)$
$\boldsymbol{P}_s(t)$	$\boldsymbol{P}_s(t) = \boldsymbol{P}_s(t-1) - \boldsymbol{L}_s(t)\boldsymbol{\chi}_s^{\mathrm{T}}(t)$	n_1^2	n_1^2
$\hat{\theta}_n(t)$	$\hat{\theta}_n(t) = \hat{\theta}_n(t-1) + L_n(t)e(t)$	n_2	n_2
$L_n(t)$	$L_n(t) = \chi_n(t)[1 + \hat{\varphi}_n(t)\chi_n(t)]^{-1}$	n_0	n_0
	$\chi_n(t) := P_n(t-1)\hat{\varphi}_n(t)$	n_2^2	$n_2(n_2-1)$
$P_n(t)$	$P_n(t) = P_n(t-1) - L_n(t)\chi_n(t)$	n_2^2	n_2^2
$\hat{v}(t)$	$\hat{v}(t) = y(t) - \hat{\boldsymbol{\varphi}}^{\mathrm{T}}(t)\hat{\boldsymbol{\theta}}(t)$	n_0	n_0
Sum		$2n_1^2 + 2n_2^2 + 3n_0 + 3n_1 + n_2$	$2n_1^2 + 2n_2^2 + 3n_0 + n_1$
Total flops		$N_2 := 4n_1^2 + 4n_2^2 + 6n_0 + 4n_1 + n_2$	

The computational efficiency of the 2S-RGELS algorithm is shown in Table 2. The computation procedures of the 2S-RELS algorithm in (43)–(51) are listed in the following.

1) Initialize: let $t = 3$, $\hat{\boldsymbol{\theta}}_s(0) = 1_2/p_0$, $\boldsymbol{P}_s(0) = p_0\boldsymbol{I}_2$, $\hat{\theta}_n(0) = 1/p_0$, $P_n(0) = p_0$, $\hat{v}(t-1) = 0$, and p_0 is taken to be a large number, e.g., $p_0 = 10^6$.
2) Collect the output data $y(t)$. Form $\boldsymbol{\varphi}_s(t)$ and $\hat{\boldsymbol{\varphi}}_n(t)$ by (50) and (51), respectively.
3) Compute the gain vector $\boldsymbol{L}_s(t)$ and the covariance matrix $\boldsymbol{P}_s(t)$ by (45) and (46). Compute the gain vector $L_n(t)$ and the covariance matrix $P_n(t)$ by (47) and (48).
4) Update the parameter estimates $\hat{\boldsymbol{\theta}}_s(t)$ and $\hat{\theta}_n(t)$ by (43) and (44), respectively.
5) Compute $\hat{v}(t)$ by (49).
6) Increase t by 1 and go to Step 2.

The computational efficiency is usually counted by the flop (the floating point operation). Here, an addition, a multiplication, a subtraction, a division all is a flop. In general, a division is considered as a multiplication and a subtraction is considered as an addition. Thus, the computational amount of an identification algorithm can be expressed by adds and multiplications. From Table 1 and 2, the total flop numbers of the RELS algorithm and the 2S-RELS algorithm are $N_1 = 4n_0^2 + 8n_0$ and $N_2 = 4n_1^2 + 4n_2^2 + 6n_0 + 4n_1 + n_2$, respectively. The flop ratio of the RELS algorithm and 2S-RELS algorithm is:

$$\frac{N_1}{N_2} = 1 + \frac{2n_1(4n_2 - 1) + n_2}{N_2} > 1.$$

$N_1 > N_2$ means that the 2S-RELS algorithm is more flop-efficient than the RELS algorithm, so the convergence speed of the 2S-RELS algorithm is faster than the RELS algorithm. For high order wave disturbance models, such as: $n_1 = 10$ and $n_2 = 9$, we can get $N_1 = 1596$, $N_2 = 887$, $N_1 - N_2 = 709$ and $\frac{N_1 - N_2}{N_1} \approx 44.42\%$. Compared with the RELS algorithm, the computation of the 2S-RELS algorithm is reduced by 44.42%.

V. WAVE PEAK FREQUENCY CALCULATION

Based on section II, section III and section IV, the wave peak frequency can be calculated on-line from a_i by transforming the roots $z_i (i = 1, 2)$ of the discrete-time equation

$$A(z) = 1 + a_1 z^{-1} + a_2 z^{-2} = 0, \tag{52}$$

to the continuous-time domain by

$$z_i = \exp(hs_i) \Longrightarrow s_i = \frac{1}{h}\ln z_i, \tag{53}$$

where s_i $(i = 1, 2)$ is the continuous-time pole locations and h is the sampling time. This yields a complex conjugate pair $s_{1,2}$ corresponding to the pole locations of the 2nd-order linear wave disturbance model, that is:

$$s_{1,2} = -\alpha \pm j\beta, \tag{54}$$

where $\alpha = \xi\hat{\omega}_0$ and $\beta = \hat{\omega}_0\sqrt{1-\xi^2}$. Hence, the wave peak frequency estimate is:

$$\hat{\omega}_0 = |s_{1,2}| = \sqrt{\alpha^2 + \beta^2}. \tag{55}$$

VI. SIMULATION RESULTS AND ANALYSIS

To acquire the input-output data for the wave peak frequency identification, a ship heading control system is constructed as seen in Figure 2. It is common to select the Nomoto model for the ship heading control system design and the Nomoto model can be written as the following transfer function:

$$\frac{r(s)}{\delta(s)} = \frac{K}{1 + Ts}, \tag{56}$$

where T and K are the maneuverability indices of a ship and δ is the input rudder angle. For the convenience of controller

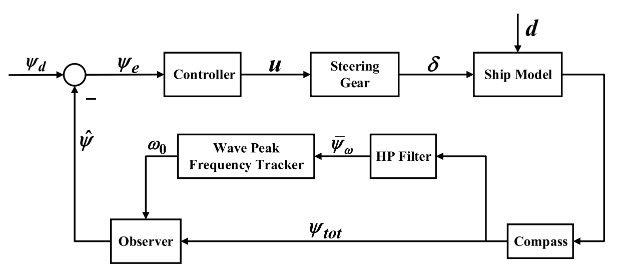

FIGURE 2. Ship heading control system.

design, let $\boldsymbol{x} := [\psi, r]^{\mathrm{T}}$, $u := \delta$ and then, the state space model can be obtained as:

$$\dot{\boldsymbol{x}} = \boldsymbol{A}\boldsymbol{x} + \boldsymbol{B}u, \tag{57}$$

where

$$\boldsymbol{A} := \begin{bmatrix} 0 & 1 \\ 0 & -\dfrac{1}{T} \end{bmatrix}, \quad \boldsymbol{B} := \begin{bmatrix} 0 \\ \dfrac{K}{T} \end{bmatrix}.$$

The linear quadratic regulator (LQR) method is applied to design the controller. Define the quadratic cost function as:

$$J_4(t) := \frac{1}{2}\int_0^t (\boldsymbol{x}^{\mathrm{T}}\boldsymbol{Q}\boldsymbol{x} + u^{\mathrm{T}}Ru)dt, \tag{58}$$

where $\boldsymbol{Q}$ is the weighted matrix of the state variable and R is the weighted value of the input variable. For minimizing the cost function of the system, the optimal control input is obtained as:

$$u = -R^{-1}\boldsymbol{B}^{\mathrm{T}}\boldsymbol{P}\boldsymbol{x}, \tag{59}$$

where the positive definite symmetric matrix $\boldsymbol{P}$ should be found by solving the algebraic Riccati equation:

$$\boldsymbol{A}^{\mathrm{T}}\boldsymbol{P} + \boldsymbol{P}\boldsymbol{A} - \boldsymbol{P}\boldsymbol{B}R^{-1}\boldsymbol{B}^{\mathrm{T}}\boldsymbol{P} + \boldsymbol{Q} = 0. \tag{60}$$

To verify the validity of the proposed algorithms, an observer is introduced and the model used for observer design is:

$$\dot{\zeta}_\omega = \psi_\omega, \tag{61}$$
$$\dot{\psi}_\omega = -\omega_0^2\zeta_\omega - 2\xi\omega_0\zeta_\omega + w_1, \tag{62}$$
$$\dot{\psi} = r, \tag{63}$$
$$\dot{r} = -\frac{1}{T}r + \frac{K}{T}\delta + w_r, \tag{64}$$

where ζ_ω is the wave state and w_1, w_r are the Gaussian white noises. By combining the ship model and the wave disturbance model, the measurement equation can be expressed as:

$$y = \psi + \psi_\omega + v, \tag{65}$$

where v is the measurement noise. The resulting state space model is:

$$\dot{\boldsymbol{x}_o} = \boldsymbol{A}_o\boldsymbol{x}_o + \boldsymbol{b}u + \boldsymbol{E}\boldsymbol{w}, \tag{66}$$
$$y = \boldsymbol{h}^{\mathrm{T}}\boldsymbol{x}_o + v, \tag{67}$$

where

$$\boldsymbol{x}_o := [\zeta_\omega, \psi_\omega, \psi, r]^{\mathrm{T}},$$
$$u = \delta,$$
$$w := [w_1, w_r]^{\mathrm{T}},$$
$$\boldsymbol{A}_o := \left[\begin{array}{cc|cc} 0 & 1 & 0 & 0 \\ -\omega_0^2 & 2\xi\omega_0^2 & 0 & 0 \\ \hline 0 & 0 & 0 & 1 \\ 0 & 0 & 0 & -\dfrac{1}{T} \end{array}\right], \quad \boldsymbol{b} := \left[\begin{array}{c} 0 \\ 0 \\ \hline 0 \\ \dfrac{K}{T} \end{array}\right],$$

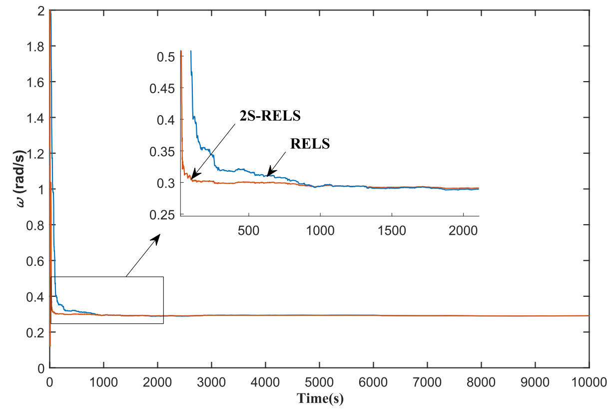

FIGURE 3. The identification results of wave peak frequency $\omega_{01} = 0.3$.

$$\boldsymbol{E} := \left[\begin{array}{c|c} 0 & 0 \\ 1 & 0 \\ \hline 0 & 0 \\ 0 & 1 \end{array}\right], \quad \boldsymbol{h}^{\mathrm{T}} := \begin{bmatrix} 0 & 1 & 1 & 0 \end{bmatrix}.$$

Neglecting the Gaussian white noise, an observer copying the ship dynamic model is:

$$\dot{\hat{\boldsymbol{x}_o}} = \boldsymbol{A}_o\hat{\boldsymbol{x}_o} + \boldsymbol{b}u + \boldsymbol{k}^{\mathrm{T}}(y - \hat{y}), \tag{68}$$
$$\hat{y} = \boldsymbol{h}^{\mathrm{T}}\hat{\boldsymbol{x}_o}, \tag{69}$$

where $\hat{\boldsymbol{x}_o}$ and $\hat{y}$ are the estimates of $\boldsymbol{x}_o$ and y, respectively and $\boldsymbol{k}^T$ is the observer gain vector which can be chosen as:

$$\boldsymbol{k} := \begin{bmatrix} K_1 \\ K_2 \\ K_3 \\ K_4 \end{bmatrix} = \begin{bmatrix} -2\omega_0(1-\xi)/\omega_c \\ 2\omega_0(1-\xi) \\ \omega_c \\ K_4 \end{bmatrix},$$

where $\omega_c > \omega_0$ is the filter cut-off frequency. The identified wave peak frequency can be used to design the observer.

The simulation model is a cargo ship with $K = 0.185(s^{-1})$, $T = 107.3(s)$ [3]. According to [4], the relative damping ratio ξ is chosen as 0.1 and the wave peak frequency ω_{0i} $(i = 1, 2, 3)$ is selected as 0.3, 0.6 and 0.9, respectively. The preset heading angle is set as 30°. In practical, the nonlinear feature of steering servomechanism must be considered due to its unneglectable influence on the heading control system. Hence, constraints were introduced for the rudder servo model in the simulation. The maximum steering angle is set as ±35° and the maximum steering rate is set as ±5°/s.

The simulation results in Figures 3–5 show that both the RELS algorithm and the 2S-RELS algorithm could estimate the wave peak frequency accurately. To evaluate the convergence speed, the RELS algorithm and the 2S-RELS algorithm are compared under the same simulation conditions. As seen in Figures 3–5, the 2S-RELS algorithm using the hierarchical identification principle has faster convergence speed than the RELS algorithm and can reduce the computational burden effectively.

In order to evaluate the performance of the proposed algorithms, a filter based on the wave peak frequency tracker

TABLE 3. The wave peak frequency estimates and estimation accuracy of the 2S-RELS algorithm.

t	$\hat{\omega_{01}}$	δ_1	$\hat{\omega_{02}}$	δ_2	$\hat{\omega_{03}}$	δ_3
100	0.25880	86.26693	0.43524	72.54039	1.01323	87.41868
200	0.26842	89.47395	0.50114	83.52333	0.93697	95.89168
500	0.28249	94.16426	0.60795	98.67467	0.92251	97.49923
1000	0.29224	97.41197	0.59831	99.71892	0.90506	99.43804
2000	0.30016	99.94568	0.59523	99.20508	0.88791	98.65704
3000	0.30701	97.66214	0.59063	98.43916	0.88360	98.17761
True values	0.3		0.6		0.9	

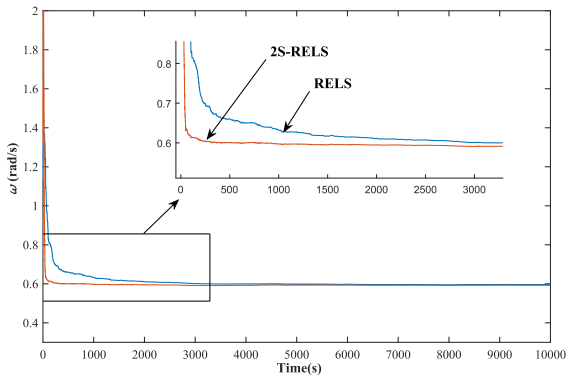

FIGURE 4. The identification results of wave peak frequency $\omega_{02} = 0.6$.

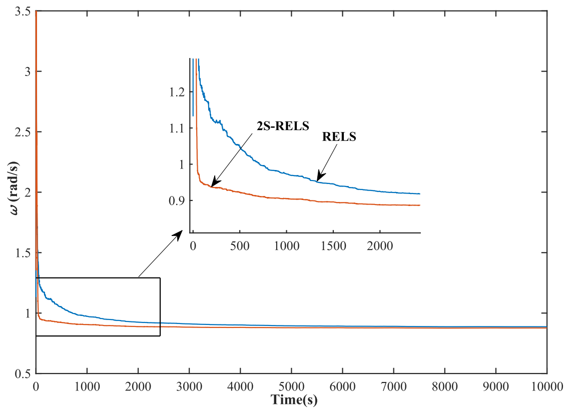

FIGURE 5. The identification results of wave peak frequency $\omega_{03} = 0.9$.

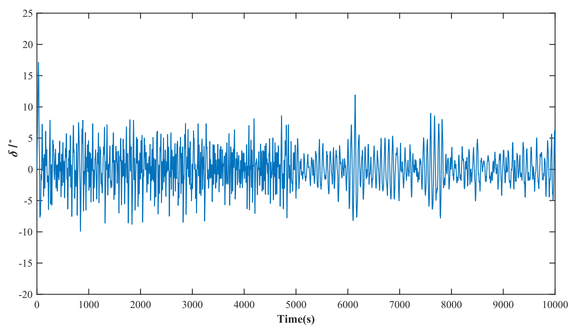

FIGURE 6. The simulation results of input rudder angle at $\omega_{01} = 0.3$.

is activated at 5000s. Figures 6–8 show that the response frequency and amplitude of the input rudder angle are reduced obviously after 5000s.

The wave peak frequency estimates $\hat{\omega_{0i}}$ and the estimation accuracy δ_i $(i = 1, 2, 3)$ of the 2S-RELS algorithm are given in Table 3, where $\delta_i = (1 - \frac{|\hat{\omega_{0i}} - \omega_{0i}|}{\omega_{0i}}) \times 100\%$. In the case of

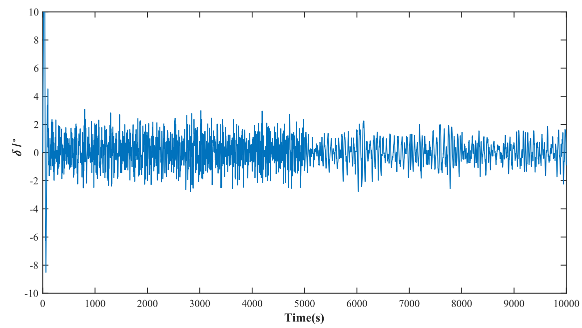

FIGURE 7. The simulation results of input rudder angle at $\omega_{02} = 0.6$.

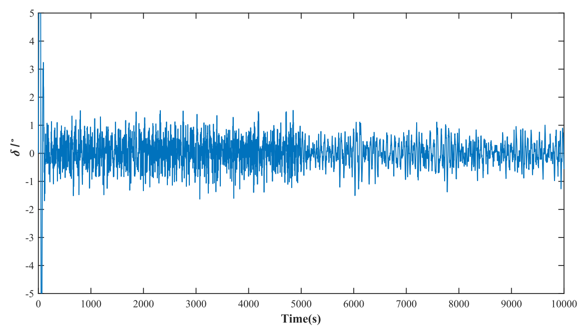

FIGURE 8. The simulation results of input rudder angle at $\omega_{03} = 0.9$.

the irregular waves, the estimation accuracy of the proposed 2S-RELS algorithm is more than 97%, which is higher than the estimation accuracy in [8]. Hence, the proposed 2S-RELS algorithm is more effective.

VII. CONCLUSION

In this paper, a RELS algorithm and a 2S-RELS algorithm are proposed to identify the wave peak frequency. In order to verify the performance of the proposed algorithms, a ship heading control system is constructed using the wave peak frequency tracker. An ARMA model is introduced as the identification model by converting the HF wave disturbance model to the input-output representation. A RELS algorithm is proposed to track the wave peak frequency by using the auxiliary model identification idea. Moreover, in order to improve the convergence speed, a 2S-RELS algorithm is proposed by using the hierarchical identification principle. Numerical simulations are carried out to evaluate the performance of the proposed algorithms. The simulation results verify the effectiveness of the proposed algorithms and compared with the methods presented in other papers [6]–[8], the proposed 2S-RELS algorithm has higher estimation accuracy. The proposed schemes in this paper can be used to design the adaptive wave filter for ship autopilot and dynamic positioning systems. The proposed two-stage recursive extended least squares algorithms can be extended to other linear systems and nonlinear systems [52]–[56] and can be applied to other fields [57]–[61] such as information processing and engineering application systems [62]–[66] and so on.

REFERENCES

[1] N. E. Kahveci and P. A. Ioannou, "Adaptive steering control for uncertain ship dynamics and stability analysis," *Automatica*, vol. 49, no. 3, pp. 685–697, Mar. 2013.

[2] T. I. Fossen, *Guidance and Control of Ocean Vehicles*. New York, NY, USA: Wiley, 1994.

[3] T. I. Fossen, *Marine Control Systems: Guidance, Navigation and Control of Ships, Rigs and Underwater Vehicles*. Trondheim, Norway: Marine Cybernetics, 2002.

[4] T. I. Fossen, *Handbook of Marine Craft Hydrodynamics and Motion Control*. Chichester, U.K.: Wiley, 2011.

[5] Y. Wang, S. Chai, and H. D. Nguyen, "Unscented Kalman filter trained neural network control design for ship autopilot with experimental and numerical approaches," *Appl. Ocean Res.*, vol. 85, pp. 162–172, Apr. 2019.

[6] T. H. Bryne, T. I. Fossen, and T. A. Johansen, "Design of inertial navigation systems for marine craft with adaptive wave filtering aided by triple-redundant sensor packages," *Int. J. Adapt. Control Signal Process.*, vol. 31, no. 4, pp. 522–544, Apr. 2017.

[7] D. J. Belleter, D. A. Breu, T. I. Fossen, and H. Nijmeijer, "A globally κ-exponentially stable nonlinear observer for the wave encounter frequency," *IFAC Proc. Vol.*, vol. 46, no. 33, pp. 209–214, 2013.

[8] D. J. W. Belleter, R. Galeazzi, and T. I. Fossen, "Experimental verification of a global exponential stable nonlinear wave encounter frequency estimator," *Ocean Eng.*, vol. 97, pp. 48–56, Mar. 2015.

[9] L. Xu and F. Ding, "Recursive least squares and multi-innovation stochastic gradient parameter estimation methods for signal modeling," *Circuits, Syst., Signal Process.*, vol. 36, no. 4, pp. 1735–1753, Apr. 2017.

[10] L. Xu, "The damping iterative parameter identification method for dynamical systems based on the sine signal measurement," *Signal Process.*, vol. 120, pp. 660–667, Mar. 2016.

[11] L. Xu and F. Ding, "Parameter estimation algorithms for dynamical response signals based on the multi-innovation theory and the hierarchical principle," *IET Signal Process.*, vol. 11, no. 2, pp. 228–237, Apr. 2017.

[12] L. Xu, F. Ding, and Q. Zhu, "Hierarchical Newton and least squares iterative estimation algorithm for dynamic systems by transfer functions based on the impulse responses," *Int. J. Syst. Sci.*, vol. 50, no. 1, pp. 141–151, Jan. 2019.

[13] J. Ding, Z. X. Cao, J. Z. Chen, and G. P. Jiang, "Recursive and iterative least squares parameter estimation algorithms for multiple-input–output-error systems with autoregressive noise," *Circuits, Syst., Signal Process.*, vol. 37, no. 5, pp. 1884–1906, May 2018.

[14] L. Wang and Y. He, "Recursive least squares parameter estimation algorithms for a class of nonlinear stochastic systems with colored noise based on the auxiliary model and data filtering," *IEEE Access*, vol. 7, pp. 181295–181304, 2019.

[15] F. Ding, "Combined state and least squares parameter estimation algorithms for dynamic systems," *Appl. Math. Model.*, vol. 38, no. 1, pp. 403–412, Jan. 2014.

[16] M. Li and X. Liu, "Auxiliary model based least squares iterative algorithms for parameter estimation of bilinear systems using interval-varying measurements," *IEEE Access*, vol. 6, pp. 21518–21529, 2018.

[17] Y. Wang and F. Ding, "The auxiliary model based hierarchical gradient algorithms and convergence analysis using the filtering technique," *Signal Process.*, vol. 128, pp. 212–221, Nov. 2016.

[18] C. Wang and T. Tang, "Recursive least squares estimation algorithm applied to a class of linear-in-parameters output error moving average systems," *Appl. Math. Lett.*, vol. 29, pp. 36–41, Mar. 2014.

[19] J. Chen, Y. Zhang, and R. Ding, "Auxiliary model based multi-innovation algorithms for multivariable nonlinear systems," *Math. Comput. Model.*, vol. 52, nos. 9–10, pp. 1428–1434, Nov. 2010.

[20] X. Zhang, F. Ding, L. Xu, and E. Yang, "State filtering-based least squares parameter estimation for bilinear systems using the hierarchical identification principle," *IET Control Theory Appl.*, vol. 12, no. 12, pp. 1704–1713, Aug. 2018.

[21] F. Ding, "Hierarchical estimation algorithms for multivariable systems using measurement information," *Inf. Sci.*, vol. 277, pp. 396–405, Sep. 2014.

[22] C. Guo, L. Wang, and F. Deng, "The auxiliary model based hierarchical estimation algorithms for bilinear stochastic systems with colored noises," *Int. J. Control, Autom. Syst.*, vol. 18, no. 3, pp. 650–660, Mar. 2020.

[23] F. Ding, H. Chen, L. Xu, J. Dai, Q. Li, and T. Hayat, "A hierarchical least squares identification algorithm for Hammerstein nonlinear systems using the key term separation," *J. Franklin Inst.*, vol. 355, no. 8, pp. 3737–3752, May 2018.

[24] V. Hassani, A. M. Pascoal, A. P. Aguiar, and M. Athans, "A multiple model adaptive wave filter for dynamic ship positioning," *IFAC Proc. Volumes*, vol. 43, no. 20, pp. 120–125, Sep. 2010.

[25] F. Deng, H.-L. Yang, L.-J. Wang, and W.-M. Yang, "UKF based nonlinear offset-free model predictive control for ship dynamic positioning under stochastic disturbances," *Int. J. Control, Autom. Syst.*, vol. 17, no. 12, pp. 3079–3090, Dec. 2019.

[26] D. Garcia, Y. Valeriano, L. Hernandez, and A. Martinez, "Wave filtering for heading control of an AUV based on passive observer," *Indian J. Mar. Sci.*, vol. 41, no. 6, pp. 540–549, 2012.

[27] F. Deng, H.-L. Yang, and L.-J. Wang, "Adaptive unscented Kalman filter based estimation and filtering for dynamic positioning with model uncertainties," *Int. J. Control, Autom. Syst.*, vol. 17, no. 3, pp. 667–678, Mar. 2019.

[28] W. Xian-Zhou and X. Han-Zhen, "Robust autopilot with wave filter for ship steering," *J. Mar. Sci. Appl.*, vol. 5, no. 2, pp. 24–29, Jun. 2006.

[29] T. Lauvdal and T. I. Fossen, "Robust adaptive ship autopilot with wave filter and integral action," *Int. J. Adapt. Control Signal Process.*, vol. 12, no. 8, pp. 605–622, Dec. 1998.

[30] J. Du, X. Hu, H. Liu, and C. L. P. Chen, "Adaptive robust output feedback control for a marine dynamic positioning system based on a high-gain observer," *IEEE Trans. Neural Netw. Learn. Syst.*, vol. 26, no. 11, pp. 2775–2786, Nov. 2015.

[31] S. Das and S. E. Talole, "Robust steering autopilot design for marine surface vessels," *IEEE J. Ocean. Eng.*, vol. 41, no. 4, pp. 913–922, Oct. 2016.

[32] D. Belleter, M. A. Maghenem, C. Paliotta, and K. Y. Pettersen, "Observer based path following for underactuated marine vessels in the presence of ocean currents: A global approach," *Automatica*, vol. 100, pp. 123–134, Feb. 2019.

[33] T. I. Fossen and T. Perez, "Kalman filtering for positioning and heading control of ships and offshore rigs," *IEEE Control Syst.*, vol. 29, no. 6, pp. 32–46, Dec. 2009.

[34] F. Deng, L.-J. Wang, and D.-M. Jiao, "Adaptive observer based backstepping controller design for dynamic ship positioning," *China Ocean Eng.*, vol. 31, no. 5, pp. 639–645, Oct. 2017.

[35] Y. Yang, J. Du, H. Liu, C. Guo, and A. Abraham, "A trajectory tracking robust controller of surface vessels with disturbance uncertainties," *IEEE Trans. Control Syst. Technol.*, vol. 22, no. 4, pp. 1511–1518, Jul. 2014.

[36] J. Guerrero, J. Torres, V. Creuze, and A. Chemori, "Adaptive disturbance observer for trajectory tracking control of underwater vehicles," *Ocean Eng.*, vol. 200, pp. 107080–107092, Mar. 2020.

[37] F. Ding, X. Zhang, and L. Xu, "The innovation algorithms for multivariable state-space models," *Int. J. Adapt. Control Signal Process.*, vol. 33, no. 11, pp. 1601–1608, Nov. 2019.

[38] F. Ding, L. Xu, D. Meng, X.-B. Jin, A. Alsaedi, and T. Hayat, "Gradient estimation algorithms for the parameter identification of bilinear systems using the auxiliary model," *J. Comput. Appl. Math.*, vol. 369, May 2020, Art. no. 112575.

[39] Y. Ji, C. Zhang, Z. Kang, and T. Yu, "Parameter estimation for block-oriented nonlinear systems using the key term separation," *Int. J. Robust Nonlinear Control*, vol. 30, no. 9, pp. 3727–3752, Jun. 2020.

[40] Y. Ji, X. Jiang, and L. Wan, "Hierarchical least squares parameter estimation algorithm for two-input Hammerstein finite impulse response systems," *J. Franklin Inst.*, vol. 357, no. 8, pp. 5019–5032, May 2020.

[41] F. Ding, Y. J. Liu, and B. Bao, "Gradient based and least squares based iterative estimation algorithms for multi-input multi-output systems," *Proc. Inst. Mech. Eng., I, J. Syst. Control Eng.*, vol. 226, no. 1, pp. 43–55, Feb. 2012.

[42] Y. Fan and X. Liu, "Two-stage auxiliary model gradient-based iterative algorithm for the input nonlinear controlled autoregressive system with variable-gain nonlinearity," *Int. J. Robust Nonlinear Control*, vol. 30, no. 14, pp. 5492–5509, Sep. 2020.

[43] X. Zhang and F. Ding, "Adaptive parameter estimation for a general dynamical system with unknown states," *Int. J. Robust Nonlinear Control*, vol. 30, no. 4, pp. 1351–1372, Mar. 2020.

[44] X. Zhang, F. Ding, and L. Xu, "Recursive parameter estimation methods and convergence analysis for a special class of nonlinear systems," *Int. J. Robust Nonlinear Control*, vol. 30, no. 4, pp. 1373–1393, Mar. 2020.

[45] L. Wang, Y. Ji, L. Wan, and N. Bu, "Hierarchical recursive generalized extended least squares estimation algorithms for a class of nonlinear stochastic systems with colored noise," *J. Franklin Inst.*, vol. 356, no. 16, pp. 10102–10122, Nov. 2019.

[46] L. Wang, Y. Ji, H. Yang, and L. Xu, "Decomposition-based multiinnovation gradient identification algorithms for a special bilinear system based on its input-output representation," *Int. J. Robust Nonlinear Control*, vol. 30, no. 9, pp. 3607–3623, Jun. 2020.

[47] X. Zhang and F. Ding, "Recursive parameter estimation and its convergence for bilinear systems," *IET Control Theory Appl.*, vol. 14, no. 5, pp. 677–688, Mar. 2020.

[48] Y. Gu, Q. Zhu, and H. Nouri, "Bias compensation-based parameter and state estimation for a class of time-delay non-linear state-space models," *IET Control Theory Appl.*, vol. 14, no. 15, pp. 2176–2185, Oct. 2020.

[49] X. Zhang, Q. Liu, F. Ding, A. Alsaedi, and T. Hayat, "Recursive identification of bilinear time-delay systems through the redundant rule," *J. Franklin Inst.*, vol. 357, no. 1, pp. 726–747, Jan. 2020.

[50] F. Ding, L. Lv, J. Pan, X. Wan, and X.-B. Jin, "Two-stage gradient-based iterative estimation methods for controlled autoregressive systems using the measurement data," *Int. J. Control, Autom. Syst.*, vol. 18, no. 4, pp. 886–896, Apr. 2020.

[51] N. Bu, J. Pang, and M. Deng, "Robust fault tolerant tracking control for the multi-joint manipulator based on operator theory," *J. Franklin Inst.*, vol. 357, no. 5, pp. 2696–2714, Mar. 2020.

[52] Y. Gu, J. Liu, X. Li, Y. Chou, and Y. Ji, "State space model identification of multirate processes with time-delay using the expectation maximization," *J. Franklin Inst.*, vol. 356, no. 3, pp. 1623–1639, Feb. 2019.

[53] Y. Gu, Y. Chou, J. Liu, and Y. Ji, "Moving horizon estimation for multirate systems with time-varying time-delays," *J. Franklin Inst.*, vol. 356, no. 4, pp. 2325–2345, Mar. 2019.

[54] L. Xu, F. Ding, X. Lu, L. Wan, and J. Sheng, "Hierarchical multi-innovation generalised extended stochastic gradient methods for multivariable equation-error autoregressive moving average systems," *IET Control Theory Appl.*, vol. 14, no. 10, pp. 1276–1286, Jul. 2020.

[55] Y. Zhou and F. Ding, "Modeling nonlinear processes using the radial basis function-based state-dependent autoregressive models," *IEEE Signal Process. Lett.*, vol. 27, pp. 1600–1604, 2020.

[56] L. Xu, F. Ding, L. Wan, and J. Sheng, "Separable multi-innovation stochastic gradient estimation algorithm for the nonlinear dynamic responses of systems," *Int. J. Adapt. Control Signal Process.*, vol. 34, no. 7, pp. 937–954, Jul. 2020.

[57] J. Pan, H. Ma, X. Zhang, Q. Liu, F. Ding, Y. Chang, and J. Sheng, "Recursive coupled projection algorithms for multivariable output-error-like systems with coloured noises," *IET Signal Process.*, vol. 14, no. 7, pp. 455–466, Sep. 2020.

[58] L. Xu, W. Xiong, A. Alsaedi, and T. Hayat, "Hierarchical parameter estimation for the frequency response based on the dynamical window data," *Int. J. Control, Autom. Syst.*, vol. 16, no. 4, pp. 1756–1764, Aug. 2018.

[59] J. Pan, X. Jiang, X. Wan, and W. Ding, "A filtering based multi-innovation extended stochastic gradient algorithm for multivariable control systems," *Int. J. Control, Autom. Syst.*, vol. 15, no. 3, pp. 1189–1197, Jun. 2017.

[60] L. Xu and G. Song, "A recursive parameter estimation algorithm for modeling signals with multi-frequencies," *Circuits, Syst., Signal Process.*, vol. 39, no. 8, pp. 4198–4224, Aug. 2020.

[61] X. Zhang and F. Ding, "Hierarchical parameter and state estimation for bilinear systems," *Int. J. Syst. Sci.*, vol. 51, no. 2, pp. 275–290, 2020.

[62] F. Ji, L. Liao, T. Wu, C. Chang, and M. Wang, "Self-reconfiguration batteries with stable voltage during the full cycle without the DC-DC converter," *J. Energy Storage*, vol. 28, Apr. 2020, Art. no. 101213.

[63] X. Zhang, F. Ding, L. Xu, and E. Yang, "Highly computationally efficient state filter based on the delta operator," *Int. J. Adapt. Control Signal Process.*, vol. 33, no. 6, pp. 875–889, Jun. 2019.

[64] Y. Zhang, Z. Yan, C. C. Zhou, T. Z. Wu, and Y. Y. Wang, "Capacity allocation of HESS in micro-grid based on ABC algorithm," *Int. J. Low-Carbon Technol.*, vol. 15, no. 4, pp. 496–505, Nov. 2020, doi: 10.1093/ijlct/ctaa014.

[65] X. Zhang, F. Ding, and E. Yang, "State estimation for bilinear systems through minimizing the covariance matrix of the state estimation errors," *Int. J. Adapt. Control Signal Process.*, vol. 33, no. 7, pp. 1157–1173, Jul. 2019.

[66] Z. Zhao, X. Wang, P. Yao, and Y. Bai, "A health performance evaluation method of multirotors under wind turbulence," *Nonlinear Dyn.*, vol. 102, no. 3, pp. 1701–1715, Nov. 2020.

JIANPING YUAN received the M.E. degree from the College of Shipbuilding Engineering, Harbin Engineering University, Harbin, China, where he is currently pursuing the Ph.D. degree in ocean engineering.

His current research interests include system identification, intelligent ship equipment and control technology, fault tolerant control, intelligent control, and hydrodynamic technology of marine vehicle.

SHUN AN received the B.E. degree from the College of Mechanical and Electrical Engineering, Qingdao University of Science and Technology, Qingdao, China, in 2019, where he is currently pursuing the M.E. degree in control science and engineering.

His current research interests include system identification, fault tolerant control, and their applications to marine surface vessels.

XINXIANG PAN received the Ph.D. degree in vehicle operation engineering from Dalian Maritime University, in 1999.

He is currently a Professor with Guangdong Ocean University. His current research interests include energy saving and emission reduction technology, safety and pollution control technologies, and their applications to marine surface vessels.

HONGFEI MAO received the Ph.D. degree in ocean engineering from Guangdong Ocean University.

He is currently a Lecturer with Guangdong Ocean University. His current research interests include interaction between waves and structures, intelligent ship equipment and control technology, intelligent control, and hydrodynamic technology of marine vehicle.

LONGJIN WANG received the Ph.D. degree in control science and engineering from Harbin Engineering University, in 2009.

From 2009 to 2013, he was an Engineer with China Shipbuilding heavy Industry Corporation. Since 2013, he has been an Associate Professor in control science and engineering with the Qingdao University of Science and Technology. His current research interests include system identification and motion control of marine crafts.